Impacts of Wind Turbine Farm Obscurations on Aircraft Escort Probability of Success

Andrew F. Wind
Defence Research and Development Canada
Centre for Operational Research and Analysis
Ottawa, ON, Canada

Joseph D. Gerber, Jacob D. Griesbach
Applied Defense Solutions
Columbia, MD, USA
jgerber@applieddefense.com
jgriesbach@applieddefense.com

***Abstract*—The presence of large wind turbine farms has been shown to significantly degrade radar tracking of aircraft. The loss in localized radar coverage could pose issues in airspace management, especially within Temporary Flight Restrictions (TFR) areas. As wind turbine development expands, there is an increasing potential that the degraded radar tracking surveillance could negatively impact safety operations. Two analytical approaches are considered to compute the probability of successfully intercepting and escorting an unauthorized aircraft away from TFR controlled areas near wind turbines. New models, which were specifically designed to address wind turbine interference with ground-based radars, are utilized to simulate both the losses in radar tracking continuity from wind turbine obscuration and the resulting impact this has on airspace safety operations. Probability distributions are used to model intercept / escort processes including interceptor take-off times. A probability of success expected value is computed for candidate routes over a range of aircraft velocities. The intercept sequences are modeled under various conditions (no turbines, existing turbines, and expected future turbine development) to measure the contrast in probability of success lost as a direct result of turbines. Both Monte Carlo and convolutional "Direct Probability" approaches are considered.**

I. Introduction

It is well known that wind turbines obscure air surveillance radar returns by smearing energy in Doppler [1,2,3,4]. Such Doppler returns can shadow or mask even strong returns from aircraft with similar range and angle characteristics [5,6,7,8]. This has sparked new debate regarding criteria for the approval of new turbine installations [9].

The work presented in this paper addresses the issue of evaluating the likelihood of successfully intercepting and escorting unauthorized aircraft away from a Temporary Flight Restrictions (TFR) area[1], while considering the effects of nearby wind turbine farms on radar tracking. Probability distributions are used to model uncertainties in the scenario timeline regarding the time required for the responding aircraft to take-off and the time required to perform escort procedures, as well as the velocity of the unauthorized aircraft.

Two methods of assessing escort probability of success are detailed within: a traditional Monte Carlo approach and a "Direct Probability" approach, where a probability distribution function is calculated for each possible velocity that rolls all of the timeline uncertainties into a single result.

To analyze the effects of wind turbine farms on air surveillance returns, the Radar Obstruction Evaluation Model / Simulator (ROEMS), developed by Analytical Graphics Inc. (AGI), is used. ROEMS computes radar equation results including wind turbine location and characteristics to determine the probability of detection for each time interval along an aircraft route. The aircraft simulator Analytical Visualization Tool (AVT), developed by Applied Defense Solutions (ADS), is utilized to generate candidate aircraft routes, emulate tracking performance from radar returns, simulate the interceptor engagement, calculate probability of success, and visualize the results.

II. Scenario Timeline

The scenario involves an unauthorized aircraft approaching a TFR area, for which the following steps must be completed: 1) *Initial Tracking* - the unauthorized aircraft is initially tracked by ground radar and identified as a potential TFR violator; 2) *Take-off* - an intercepting aircraft prepares to take-off; 3) *Fly-out* - the intercepting aircraft flies towards the unauthorized aircraft; 4) *Maneuvers* - the intercepting aircraft first uses onboard radar systems to detect the unauthorized aircraft and then maneuvers to a position near it; 5) *Escort Procedures* - the intercepting aircraft performs escort procedures to instruct the unauthorized aircraft to divert and avoid breaching the TFR. Steps 2 and 3 are also collectively termed en route. Ideally, the unauthorized pilot should understand the escort procedures (e.g. hailing and rocking wings) and comply with instructions [10].

[1] The Federal Aviation Administration (FAA) is responsible for the safety of civilian aviation. The FAA uses TFRs to restrict aircraft operation within designated areas, e.g. areas surrounding major political/sporting events, or wild fires.

978-1-4799-2035-8/14/$31.00 ©2014 Crown

To construct a "standard timeline", it is constructed in reverse from the TFR boundary back, based on a selected unauthorized aircraft velocity and a set of standard times, t_s, for the initial tracking period, take-off time, and escort procedures. The standard timeline also considers the geometry based on the unauthorized aircraft's heading and the location of the interceptor's airport. Steps 3 and 4 are calculated using AVT to perform an optimal intercept considering the intercepting aircraft's performance characteristics. Fig. 1 illustrates the scenario timeline.

A. Input Distributions

For this report, notional values are used for the inputs. In practice, real measurements could be used as the inputs for constants and to form empirical probability density functions (PDFs) for variables.

The time required for take-off is represented by a normal distribution and limited to two standard deviations. $t_{s,take-off}$, for constructing the timeline is chosen such that it represents 80% on the corresponding cumulative distribution function (CDF).

The time required to perform the escort procedures is represented by a uniform PDF. This represents a simple linear CDF where the likelihood of the unauthorized aircraft diverting is constantly increasing as further techniques are employed to gain compliance. As the interceptor progresses through a series of procedures, it is assumed that the unauthorized aircraft becomes more and more likely to respond appropriately. The maximum escort time is selected conservatively as the standard value, $t_{s,escort}$.

The unauthorized aircraft's velocity is chosen from a PDF over a range of speeds representative of aircraft operating in the airspace. These aircraft can vary from large airliners and business jets to single engine aircraft.

B. Initial Tracking

The initial tracking interval is analyzed for radar obstructions. This is accomplished by examining the ROEMS data for radar access to the unauthorized aircraft during the interval. The track initiation time, t_i, is dependent on the first opportunity, since the initial tracking interval begins, to acquire a specified period of uninterrupted radar access, t_u, of the unauthorized aircraft. Once t_i is identified, it is compared to the ending time of the standard initial tracking interval, $t_{s,track}$. The difference between the two times is understood to be the initial tracking overrun, $\beta = t_i - t_{s,track}$.

The value β modifies the standard timeline intervals, such that negative values allow for earlier take-off, maneuver, and escort times, while positive values indicate that an extended initial tracking interval was necessary and subsequent intervals will be delayed. After applying β to the standard timeline, we refer to it as the "modified timeline".

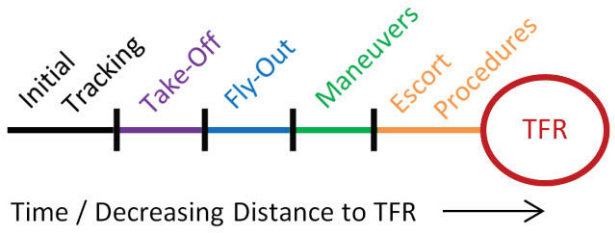

Fig. 1. Timeline for unauthorized aircraft

C. En Route Radar Coverage

The en route time interval (take-off and fly-out) is considered for radar access. A value is computed that describes the percentage of time during the interval that the radar had access to the unauthorized aircraft. This value is referred to as the en route radar coverage percentage, $P_{cov} \in [0,1]$.

D. Maneuvers radar coverage

During the maneuvers interval, the intercepting aircraft seeks to find a continuous radar coverage sub-interval of sufficient duration using its own radar to then position for escorting. Without a capability to calculate obstructions from a dynamic air platform, radar obstruction regions are estimated using a radius around each turbine. When the unauthorized aircraft flies through these obstructions, it is assumed that the intercepting aircraft radar is obstructed and loses continuous coverage.

III. Monte Carlo Analysis

For the Monte Carlo analysis, random values are drawn from the PDFs for the unauthorized aircraft velocity and take-off time. These random draws are used to first calculate the standard timeline and then adjust the modified timeline with the specific take-off time to create a "Monte Carlo timeline".

Using the Monte Carlo timeline, AVT models a new optimal en route and maneuvers flight path and calculates case specific results for P_{cov} and the maneuvers radar coverage. If the minimum continuous radar coverage cannot be achieved within the maneuvers interval, a binary probability, B_m, fails.

The modified timeline also provides the amount of time available for escort procedures. When β is positive, take-off is delayed and less time is available for escort procedures. Based on the uniform PDF, the probability of the unauthorized aircraft responding appropriately prior to the time available is described by a linear CDF, appropriately bounded between zero and one, $F_{escort}(\beta) = 1 - \beta/t_{s,escort}$.

The probability of success for a Monte Carlo trial is calculated as the product of the en route coverage, the binary maneuvers probability and the probability of the unauthorized aircraft responding to escort procedures.

$$P_{MC} = P_{cov} B_m F_{escort}(\beta) \quad (1)$$

The final probability of success, calculated over many trials is their average probability of success. Since each Monte Carlo sample is fully simulated, this can lead to an analysis that requires lots of computational power and/or time to compute.

IV. Direct Probability Analysis

An alternative analysis method is proposed that makes more efficient use of the known probability distributions, which is named Direct Probability Analysis. With this approach, the probabilities associated with take-off and escort

procedures times are effectively computed simultaneously for all possible time combinations. This leads to an analysis that can be accomplished by iterating through target velocity only, resulting in a much faster simulation.

A simplification in this approach is that it does not model every time combination and how it affects the intercepting flight paths. Instead it relies on the modified timeline to calculate a representative en route P_{cov} for all situations and a representative time interval required to maneuver into escort position.

A. Translating maneuver delays to the take-off PDF

Realizing that take-off times can vary across its PDF, intercepting aircraft could arrive earlier or later than expected compared to the modified timeline. To accommodate this, the maneuver interval, along which the unauthorized aircraft flight path radar obstructions are assessed, is extended accordingly. This extended maneuvers interval is assessed for all time intervals where the radar does not have the required minimum continuous access to the target.

In the Direct Probability analysis, a specific intercepting aircraft obtained from the set of all possibilities is delayed to account for obstructions from locating the unauthorized aircraft from the start of its maneuver interval. Once the minimum access requirement is met, the aircraft continues its maneuvers to proceed to escorting. Rather than simulating these delays in the intercepting flight paths, the delays are translated to delayed take-offs such that the aircraft should arrive as the unauthorized aircraft exits the obstructed region.

Mathematically, the take-off time PDF is modified to shift probabilities to the right (increased time) based on the lack of continuous radar coverage. For example, if the minimum continuous radar access requirement could not be met from times t_1 to t_2, then the following modifications are made to the take-off time PDF, which is denoted as $\tilde{f}_{take-off}(t)$.

$$\tilde{f}_{take-off}(t) = \begin{cases} f_{take-off}(t) & t < t_1 \\ 0 & t_1 \le t < t_2 \\ f_{take-off}(t) + \int_{t_1}^{t_2} f_{take-off}(x)\,dx & t = t_2 \\ f_{take-off}(t) & t > t_2 \end{cases} \quad (2)$$

The above modifications are repeated for each obstructed radar interval.

B. Individual probability of success

Next, the notion of effectively adding the modified PDFs together is calculated. To add the two PDFs together we use their convolution.

$$f_{sum}(t) = (\tilde{f}_{take-off} * f_{escort})(t) \quad (3)$$

Given β, the maximum time available to complete the mission, t_{max}, must be calculated to find the corresponding probability in the CDF of the sum distribution.

$$t_{max} = t_{s,track} + t_{s,take-off} + t_{s,escort} - \beta \quad (4)$$

To evaluate the probability of success for the current velocity, v, we evaluate the probability that the sum of the component distributions is less than t_{max} and scale the result by the en route radar coverage percentage. Thus,

$$P_{DP} = F_{sum}(t_{max})P_{cov} \quad (5)$$

where $F_{sum}(t)$ is the CDF of the sum distribution.

C. Final probability of success calculations

Equation (5) derives the conditional probability of success for a particular velocity selection. One may compute the overall probability of success for all desired velocities by iterating through unauthorized aircraft velocities and calculating the weighted average of each probability of success using the velocity PDF as the weights.

V. RESULTS

This section will compare the results from each approach using a fictitious scenario. Each approach is applied to three cases: where no turbines are considered as a baseline (but where terrain masking may provide obstructions); where currently built turbines are considered; and where approved and proposed turbines are added to consider a potential future.

The scenario geography is presented in Fig. 2. A 10 nautical mile radius TFR, surrounding a special event, is located to the northwest. The radar detection coverage is shown by the white outline. Intercepting aircraft are stationed further to the southwest. For this analysis, a ten degree wedge of incoming routes (red lines) approaching from the east are considered. These routes pass near turbines, both existing (blue dots) and proposed (yellow dots). In this example the flight routes are unaffected by terrain masking so the no turbine case should always succeed with full radar coverage.

As an aircraft flies near a wind turbine farm, its radar return can become obscured by the turbine clutter. An example flight route is shown in Fig. 3 to demonstrate how radar tracking is degraded. Green segments represent positive tracking of the aircraft. Orange segments demonstrate the radar track fading until it is lost if it turns red. After the wind turbine farm, the radar track is reacquired and turns green again.

Fig. 4 shows the probability of success versus unauthorized aircraft velocity for the Monte Carlo approach. A subsample of individual trial results are shown for illustration purposes. Trend lines averaged over the ten approach angles are superimposed. In general, the probability of success decreases as existing and proposed turbines are added to the analysis, degrading radar tracking with the increasing clutter. The individual results can contain zero probability trials due to several factors. The failure of the binary factor, B_m, can occur if turbines prevent sufficient radar coverage during the maneuvers interval. Alternatively, a large tracking overrun combined with drawing a large take-off value can result in insufficient time left to perform the intercept. These results are smoothed out when averaged over multiple trials and the ten approach angles.

The Direct Probability method only requires one calculation for each approach angle and velocity combination. Therefore, the Direct Probability results are presented in Fig. 5 without individual trials.

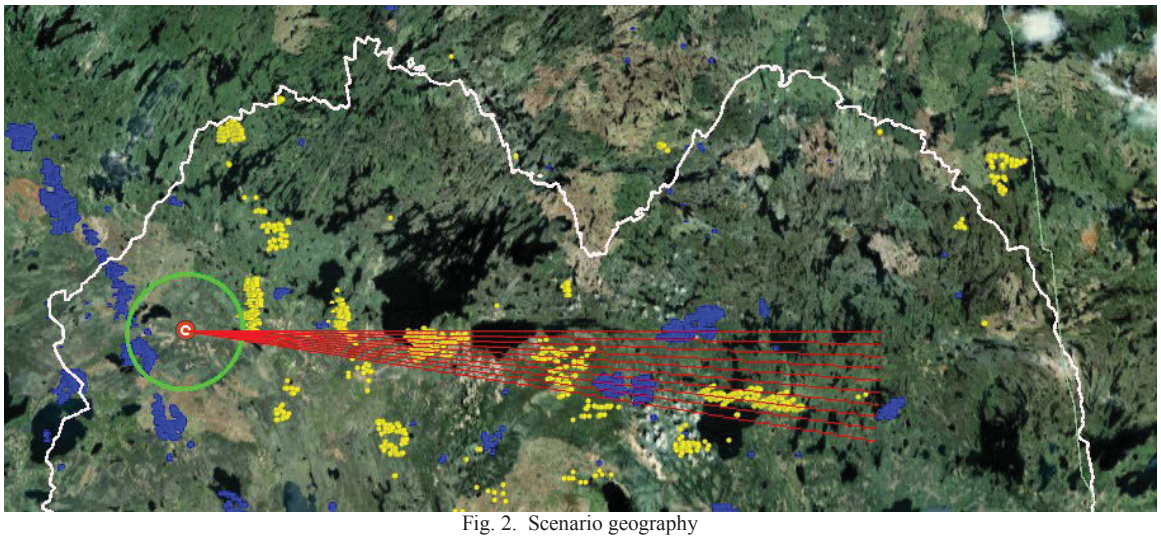

Fig. 2. Scenario geography

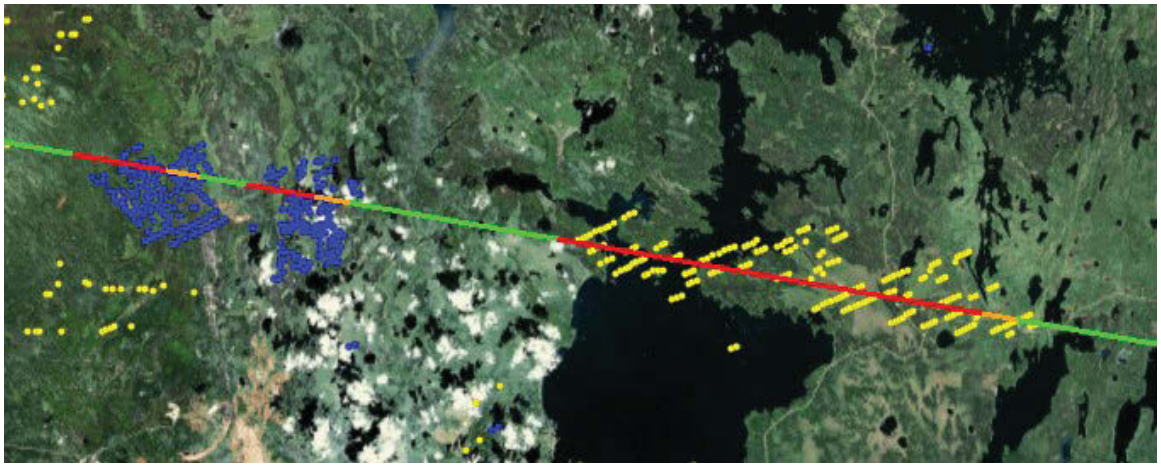

Fig. 3. Example of radar tracking along a flight route

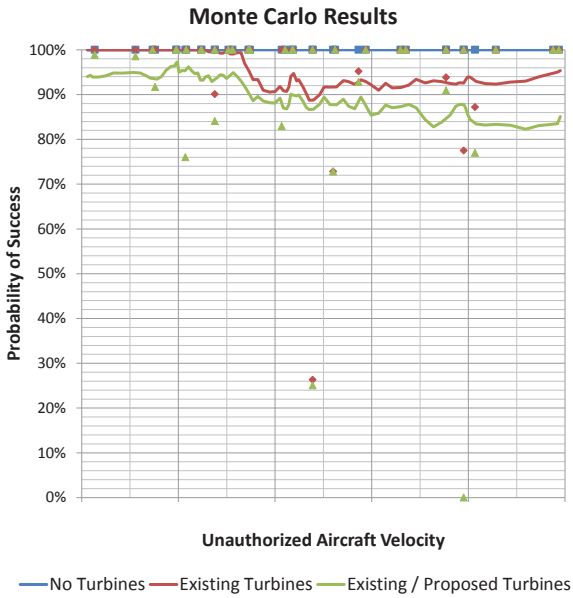

Fig. 4. Monte Carlo results averaged over all approach angles. A sample of individual trial results are also shown for illustration.

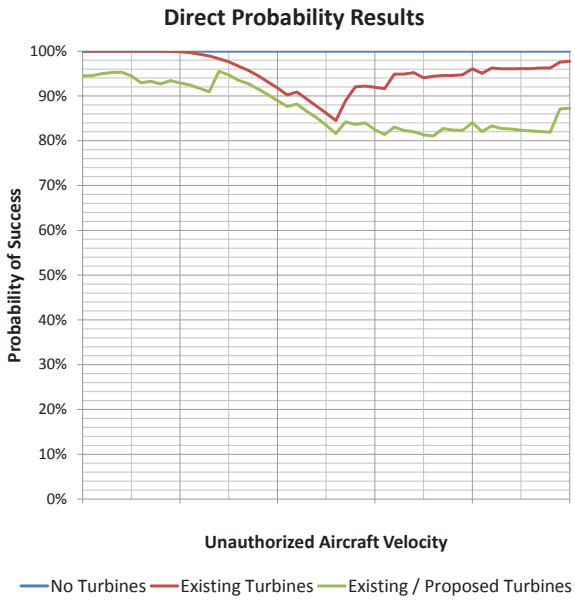

Fig. 5. Direct Probability results averaged over all approach angles

A comparison of the final results, averaged over all radials, and over all velocities is shown in Table 1. Note that the Direct Probability approach must weight each result by its likelihood of occurring from the velocity PDF. In the Monte Carlo approach, velocities were drawn from the PDF and therefore are naturally weighted in the set of trials.

TABLE I. COMPARISON OF FINAL RESULTS

Turbine Case	No Turbines	Existing	Existing & Proposed
Monte Carlo	100%	95.9%	89.8%
Direct Probability	100%	95.8%	88.9%

REFERENCES

[1] L. Danoon and A. Brown, "Modeling Methodology for Computing the Radar Cross Section and Doppler Signature of Wind Farms," IEEE Transactions on Antennas and Propogation, vol 61, no. 10, pp. 5166-5174, October 2013.

[2] F. Kong, Y. Zhang, R. Palmer, and Y. Bai, "Wind Turbine Radar Signature Characterization by Laboratory Measurements," in IEEE Radar Conference, Kansas City, MO, 2011.

[3] Y. Lok, A. Palevsky, and J. Wang, "Simulation of Radar Signal on Wind Turbine," IEEE Aerospace and Electronic Systems Magazine, pp. 39-42, August 2011.

[4] R. Ohs, G. Skidmore, and G. Bedrosian, "Modeling the Effects of Wind Turbines on Radar Returns," in Military Communications (MILCOM) Conference, San Jose, CA, 2010.

[5] G. Greving, W. Biermann, and R. Mundt, "Wind Turbines as Distorting Scaterring Objects for Radar – Visibility, Desensitization, and Shadowing," in 13th International Radar Symposium, Warsaw, Poland, 2012.

[6] C. Lute and W. Wieserman, "ASR-11 Radar Performance Assessment over a Wind Turbine Farm," in IEEE Radar Conference, Kansas City, MO, 2011.

[7] J. Perry and A. Biss, "Wind Farm Clutter Mitigation in Air Surveillance," IEEE Aerospace and Electronic Systems Magazine, vol 22, no. 7, pp. 35-40, July 2007.

[8] A. Theil and L. van Ewijk, "Radar Performance Degradation due to the Presence of Wind Turbines," in IEEE Radar Conference, Boston, MA, 2007.

[9] A. Theil, M. Schouten, and A. de Jong, "Radar and Wind Turbines: A Guide to Acceptance Criteria," in IEEE Radar Conference, Washington, DC, 2010.

[10] Federal Aviation Administration, Aeronatical Information Manual (AIM), Chapter 5, Section 6, Aug 22, 2013.